Journal of the American College of Cardiology
© 2010 by the American College of Cardiology Foundation
Published by Elsevier Inc.

Vol. 56, No. 13, 2010
ISSN 0735-1097/$36.00
doi:10.1016/j.jacc.2010.02.070

Impact of Systolic and Diastolic Deformation Indexes Assessed by Strain-Encoded Imaging to Predict Persistent Severe Myocardial Dysfunction in Patients After Acute Myocardial Infarction at Follow-Up

Mirja Neizel, MD,*† Grigorios Korosoglou, MD,* Dirk Lossnitzer, MD,* Harald Kühl, MD,‡ Rainer Hoffmann, MD,‡ Christina Ocklenburg, MSc,§ Evangelos Giannitsis, MD,* Nael F. Osman, PhD,‖¶ Hugo A. Katus, MD,* Henning Steen, MD*

Heidelberg, Düsseldorf, and Aachen, Germany; Baltimore, Maryland; and Cairo, Egypt

Objectives This study evaluated the value of systolic and diastolic deformation indexes determined by strain-encoded imaging to predict persistent severe dysfunction at follow-up in patients after reperfused acute myocardial infarction (AMI) in comparison with late gadolinium enhancement (LGE).

Background Animal studies suggest that regional diastolic function provides information about myocardial viability after AMI. However, data in humans are sparse.

Methods Twenty-six patients underwent magnetic resonance imaging 3 ± 1 days after successfully reperfused ST-segment elevation myocardial infarction and at a follow-up of 6 months. Cine, strain-encoded, and LGE images were acquired. Peak systolic circumferential strain (E_{cc}) and early diastolic strain rate (E_{cc}/s) were calculated for each segment at baseline and at follow-up. A cutoff E_{cc} value of −9% was used to define severe dysfunction at follow-up.

Results A total of 312 segments were analyzed; 119 segments showed abnormal baseline function. Thirty-five segments showed severe dysfunction at follow-up, which was defined as E_{cc} at follow-up <9%. The area under the curve for E_{cc}/s was 0.82 (95% confidence interval [CI]: 0.72 to 0.89), for E_{cc} 0.74 (95% CI: 0.64 to 0.83), and for LGE 0.85 (95% CI: 0.77 to 0.92). A comparison of receiver-operating characteristic curves demonstrates that LGE is not significantly different than E_{cc}/s but is significantly different than E_{cc} ($p = 0.32$ vs. $p < 0.05$) for prediction of severe dysfunction at follow-up.

Conclusions Regional diastolic function provides similar accuracy to predict persistent severe dysfunction at follow-up to LGE and is superior to regional systolic function in patients after AMI. Diastolic deformation indexes may serve as a new parameter for assessment of viability in patients after AMI. (SENC in AMI Study; NCT00752713). (J Am Coll Cardiol 2010;56:1056–62) © 2010 by the American College of Cardiology Foundation

Evaluation of reversible dysfunction after acute myocardial infarction (AMI) has important therapeutic and prognostic implications (1,2). Several studies have shown that late gadolinium enhancement (LGE) is a reliable method to evaluate myocardial viability (3–5). In patients after AMI, evaluation of the transmural extent of infarcted tissue defined by LGE allows prediction of improvement in contractile function (5–7). Recent experimental animal studies suggest that diastolic deformation indexes may also provide information about myocardial viability after AMI (8,9). However, if analysis of diastolic function has similar predictive power compared with LGE in patients after AMI has not been investigated so far in humans using cardiac magnetic resonance (CMR).

The state-of-the-art technique for quantification of regional function in CMR is myocardial tagging. However,

From the *Department of Cardiology, University Hospital Heidelberg, Heidelberg, Germany; †Department of Cardiology, University Hospital Düsseldorf, Düsseldorf, Germany; ‡Department of Cardiology, University Hospital Aachen, Aachen, Germany; §Department of Medical Statistics, University Hospital Aachen, Aachen, Germany; ‖Department of Radiology, Johns Hopkins University, Baltimore, Maryland; and the ¶Nile University, Cairo, Egypt. This work was supported in part by a grant from the National Institutes of Health (R01 HL072704). This paper is approved by the Conflict of Interest Committee at Johns Hopkins University. Dr. Neizel is a research fellow funded by an internal research program of the medical faculty of the University Hospital Aachen. Prof. Nael Osman is a founder and shareholder in Diagnosoft Inc. All other authors have reported that they have no relationships to disclose.

Manuscript received July 14, 2009; revised manuscript received January 8, 2010, accepted February 1, 2010.

this technique is affected by rapid fading of tags, and therefore investigations of diastolic abnormalities are difficult at least at 1.5-T. Recently, strain-encoded (SENC) imaging was introduced as a new MR technique for myocardial deformation imaging. Several studies have shown that SENC can accurately determine strain and strain rate (10–13). In addition, SENC, compared with myocardial tagging, is a method that is less affected by diastolic fading. We therefore thought that SENC may be an ideal tool to determine not only the regional systolic but also regional diastolic function.

The aim of this study was to investigate the value of systolic and diastolic deformation indexes determined by SENC imaging to predict persistent severe dysfunction at follow-up in patients after reperfused AMI. We hypothesized that regional diastolic function assessed with SENC is superior to regional systolic function and comparable to LGE.

Abbreviations and Acronyms

AMI = acute myocardial infarction
AUC = area under the curve
CMR = cardiac magnetic resonance
E_{cc} = circumferential strain
LGE = late gadolinium enhancement
MRI = magnetic resonance imaging
MVO = microvascular obstruction
PCI = percutaneous coronary intervention
RF = radiofrequency
ROC = receiver-operating characteristics
SENC = strain encoded

Methods

Patient cohort. Between June 2007 and January 2008, patients with ST-segment elevation myocardial infarction (MI) admitted to the University Hospital Heidelberg were screened. To be included in the study, the patients had to have a first-time AMI with a clearly identified culprit coronary vessel identified by coronary angiography. Moreover, patients with severe hemodynamic compromise or patients requiring inotropic support were excluded from the study. In addition, patients with contraindication to magnetic resonance imaging (MRI) or gadolinium-based contrast agent and patients who were already transferred to other hospitals at the time of possible CMR examination were excluded from the study. All patients had to have sinus rhythm to be included. Thirty patients fulfilled the inclusion criteria and were investigated at baseline. Two patients received an implantable cardioverter-defibrillator during the follow-up period and therefore were not available for follow-up CMR study. Two patients refused to participate in the follow-up study. In total, 26 patients had baseline and follow-up CMR studies.

All patients were successfully reperfused by acute percutaneous coronary intervention (PCI) with post-interventional Thrombolysis In Myocardial Infarction flow grade 3 on coronary angiography. None of the patients had a clinical event indicative of MI between acute PCI and follow-up.

The study protocol complied with the Declaration of Helsinki and was approved by the local institutional ethical committee. Written informed consent was obtained from each patient.

Imaging protocol. The CMR imaging was performed 3 ± 1 days after acute PCI and at a follow-up of 6 ± 2 months using a 1.5-T MR scanner (Achieva, Philips, Best, the Netherlands).

CINE IMAGING. Assessment of resting left ventricular function was determined by cine images using a steady-state–free precession sequence in short-axis view (10 to 12 slices covering the whole left ventricle from base to apex) and long-axis 2- and 4-chamber views (echo time [TE] 1.39 ms; repetition time [TR] 2.8 ms; flip angle 60°; spatial resolution 2.4 × 2.5 × 8 mm^3; 35 phases per cardiac cycle) with a breath-hold time of 7 to 10 s per image.

SENC IMAGING. SENC imaging is a special modification to the MR scanner software that enables the quantification of regional deformation of tissue as a result of cardiac motion. The technique produces images with intensity that depends on the degree of tissue deformation, measured by strain—which is the change in length per unit length of tissue. Therefore, the resulting anatomic images of the scanner are encoded with the strain values of the deformations. In contrast to conventional tagging, in which the tagging modulation gradient is applied in the phase- or frequency-encoding direction, the gradient is applied in the slice selection direction, parallel to the image plane, for SENC. Therefore long-axis views were used to calculate circumferential strain. Radiofrequency (RF) pulses with ramped flip angles are applied to compensate for tag fading caused by longitudinal relaxation and to maintain constant myocardial signal intensity throughout the cardiac cycle (12).

Imaging parameters of the prospectively triggered pulse sequence were a 380-mm field of view, voxel size of 4/4/10 mm^3, TR/TE 25/0.9 ms, flip angle 30° (last angle in the sequence of the RF pulses). Strain-encoded imaging as a pulse sequence has relatively lower signal-to-noise ratio than conventional cine acquisition; to supplement the loss, thicker slices (10 mm) were used. Spiral acquisition was used to perform faster image acquisition without sacrificing the signal-to-noise ratio. The temporal resolution was 25 ms, and the number of phases (typically 29 to 37) was adapted to the current heart rate to cover approximately 100% of the cardiac cycle. Strain-encoded imaging involves 2 acquisitions per slice. Both were conducted in a single threshold of 8 to 10 s.

LGE. Five and 10 min after gadolinium contrast injection LGE imaging was performed using a 3-dimensional–gradient spoiled turbo fast-field-echo sequence with an unselective 180° inversion-recovery pre-pulse triggered to end-diastole acquired in the short axis covering the whole ventricle (TR/TE 3.2/1.16 ms; flip angle 15°; spatial resolution 1.5 × 1.7 mm^2) (14,15). The acquired 10-mm–thick

slices were interpolated to 5-mm slices. The inversion time was adapted individually to suppress signal of normal myocardial tissue (typically 200 to 300 ms). The breath-hold time was 10 to 14 s.

Data analysis. For strain measurements of the long-axis views, the ventricle was divided into 12 segments (septal basal, midventricular, and apical; lateral basal, midventricular, and apical; anterior basal, midventricular, and apical; and inferior basal, midventricular, and apical).

All strain measurements were performed based on SENC images using a dedicated software (Diagnosoft MAIN, version 1.06, Diagnosoft Inc., Palo Alto, California). An example is given in Figure 1. Circumferential strain (E_{cc}) was calculated for each segment. Circumferential strain rate was used to measure regional diastolic function and was calculated by dividing the change in strain between time frames by the temporal resolution. Early diastolic circumferential strain rate (E_{cc}/s) was defined as the slope divided by the duration from end-systole to mid-diastole as has been previously published for MR tagging studies and SENC studies (10,13,16,17). A cut-off E_{cc} value of −15% at baseline determined by SENC distinguished dysfunctional segments from segments with normal function. Severe dysfunction at baseline and follow-up was defined as E_{cc} <9%.

For interpretation of contrast-enhanced images, the segmental extent of LGE on short-axis planes was calculated at baseline. The bins for LGE were determined with respect to the transmural extent of the defect. The segments were categorized on a 5-point scale according to Kim et al. (4); a score of 0 indicated no LGE, 1 indicated 1% to 25% LGE, 2 indicated 26% to 50% LGE, 3 indicated 51% to 75% LGE, and 4 indicated 76% to 100% LGE. Transmural infarcted segments with signs of microvascular obstruction (MVO) were also regarded separately in a subanalysis.

The LGE images were analyzed using short-axis views, and E_{cc} and E_{cc}/s from SENC images were analyzed using long-axis views. By using anatomic landmarks (e.g., the papillary muscle), we intended to find the same image planes.

Interobserver variability. Measurements of myocardial strain assessed with SENC were evaluated in 15 randomized patients with AMI (180 segments) by 2 independent observers unaware of wall-motion abnormalities or presence of infarcted tissue.

Statistical analysis. Data are expressed as mean ± SD. Continuous variables were compared by Student *t* test. Other comparisons were performed using a Mann-Whitney *U* test. For comparison of strain-values across different categories of transmuralities, a linear mixed model was applied to address the issue of multiple observations per patient.

Taking into account that there were 12 segments per patient to be analyzed, a generalized estimating equation approach with a binomial distribution, a logit link, and a working correlation matrix with exchangeable correlation was used to explore the ability of strain and strain rate parameters to predict severe dysfunction at follow-up. The output from this analysis allowed the derivation of receiver-operating characteristics (ROC) curves, which were used to designate cut-offs and calculate the area under the curve (AUC), sensitivities, and specificities. We chose the optimal cut-point as the cut-point associated with the highest accuracy in ROC analysis.

For comparison of ROC curves, we used the output derived from a generalized estimating equations model that took account of correlated observations within individuals for further analysis.

Interobserver variability was calculated by intraclass correlation coefficient (ICC). A p value <0.05 was regarded as

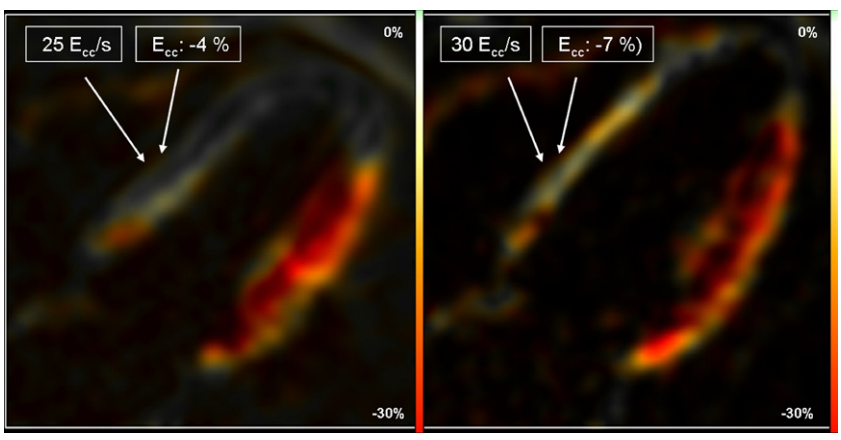

Figure 1 Example of Strain-Encoded Imaging Study

Color-coded strain-encoded image at baseline **(left)** and follow-up **(right)** of a patient with anterior myocardial infarction. The **red color** implicates maximal deformation, whereas no color implicates no deformation at all. In the segment indicated, peak systolic circumferential strain and early diastolic strain rate show no significant improvement at follow-up. E_{cc} = circumferential strain.

Table 1 Patient Characteristics (n = 26)

Age (yrs)	56 ± 10
Men/women, n	22/4
Hypertension	15 (58)
Hypercholesterolemia	9 (35)
Diabetes mellitus	3 (12)
Family history of cardiovascular disease	15 (58)
Smoking	15 (58)
EF baseline (%)	51 ± 9
Infarct size baseline (g)	38 ± 24
EF follow-up (%)	53 ± 11
Culprit lesion	
LAD	9 (35)
RCA	13 (50)
LCX	4 (15)
Medication at follow-up	
Beta-blocker	26 (100)
ACE inhibitor/ARB	25 (96)
Statin	19 (73)

Values are expressed as mean ± SD or n (%).
ACE = angiotensin-converting enzyme; ARB = angiotensin II receptor blocker; EF = ejection fraction; LAD = left anterior descending; LCX = left circumflex artery; RCA = right coronary artery.

statistically significant. Statistical analysis was performed using MedCalc (version 9.6.3, Mariakerke, Belgium) and SAS (version 9.13, SAS Institute Inc., Cary, North Carolina).

Results

Clinical baseline characteristics are given in Table 1. In total, 312 segments were analyzed. Image quality for SENC images was determined by the quality of the strain curves. If strain curves suffered too much from noise, visible as spikes instead of a strain curve, they were excluded from data analysis. For SENC analysis, 12 segments (4%) had to be excluded because of insufficient image quality. For interpretation of contrast-enhanced images, no segment had to be excluded.

At baseline, 217 segments showed no signs of LGE, 12 segments showed 0% to 25% LGE, 17 segments had 26% to 50% LGE, 18 segments had 51% to 75% LGE, and 48 segments had 76% to 100% LGE. From the 48 segments with 76% to 100% LGE, 31 segments presented with signs of MVO. A total of 119 segments showed abnormal myocardial function at baseline (68 with severe dysfunction), and 35 (29%) segments still showed severe dysfunction at follow-up.

Regional systolic and diastolic function for characterization of myocardial damage. Peak E_{cc} values and E_{cc}/s values of different transmurality states at baseline and follow-up are shown in Table 2. Regional systolic function did recover more than regional diastolic function at follow-up.

Segments that still showed severe dysfunction at follow-up had significantly different E_{cc} and E_{cc}/s values at baseline than segments with no functional recovery ($p < 0.01$ for all).

Relationship between regional diastolic function in acute state and change in regional systolic function between acute state and follow-up. In dysfunctional segments with E_{cc}/s <31, the E_{cc} at acute state was −3.1 ± 5% and −6.2 ± 2.1% at follow-up. In dysfunctional segments with E_{cc}/s >31, the E_{cc} was −8.6 ± 6.6% at acute state and −15.7 ± 4.3% at follow-up. The change of E_{cc} between acute state and follow-up was significantly higher in segments presenting with E_{cc}/s >31 ($p < 0.001$).

Comparison of regional systolic function, regional diastolic function, and delayed enhancement imaging for prediction of persistent severe myocardial dysfunction. An E_{cc} <−9% had a sensitivity of 48% and a specificity of 94% for prediction of severe myocardial dysfunction (AUC: 0.74, 95% confidence interval [CI]: 0.64 to 0.83). For regional diastolic function, a cut-off value of <31 E_{cc}/s had a sensitivity of 82% and a specificity of 75% for prediction of severe myocardial dysfunction (AUC: 0.82, 95% CI: 0.72 to 0.89). Late gadolinium enhancement >75% achieved a sensitivity of 80% and a specificity of 79% (AUC: 0.85, 95% CI: 0.77 to 0.92) (Fig. 2). In a comparison of ROC curves, LGE was significantly different than E_{cc} but not significantly different than E_{cc}/s ($p = 0.32$ vs. $p < 0.05$, respectively). A combination of E_{cc}/s and LGE achieved an AUC of 0.86 (95% CI: 0.77 to 0.93), which was not significantly different than LGE and E_{cc}/s alone.

Influence of MVO on regional systolic and diastolic function. In a comparison of hyperenhanced segments with MVO against segments without MVO, segments with MVO demonstrated significantly impaired regional systolic and diastolic function at baseline and follow-up ($p < 0.01$ for all) (Figs. 3 and 4). In segments with MVO, E_{cc} and E_{cc}/s did not significantly improve at follow-up ($p = 0.2$ and $p = 0.99$, respectively).

Table 2 Peak E_{cc} Values and E_{cc}/s Values

	E_{cc} (%)			E_{cc}/s (1/s)		
Transmurality States	Baseline	Follow-Up	p Value	Baseline	Follow-Up	p Value
0%–25% (n = 12)	−13 ± 6	−17 ± 5	NS	62 ± 48	96 ± 44	NS
26%–50% (n = 17)	−11 ± 8	−16 ± 6	NS	78 ± 48	85 ± 51	NS
51%–75% (n = 18)	−8 ± 7	−13 ± 6	<0.05	56 ± 34	56 ± 30	NS
76%–100% (n = 48)	−4 ± 6	−7 ± 6	<0.05	26 ± 35	32 ± 36	NS

Values are expressed as mean ± SD.
E_{cc} = circumferential strain.

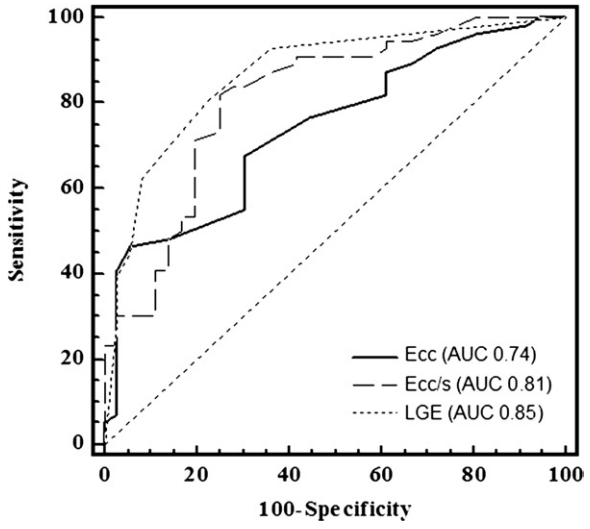

Figure 2 Prediction of Severe Persistent Dysfunction at Follow-Up

Receiver-operating characteristics curves for regional systolic (circumferential strain [E_{cc}]) and diastolic function (E_{cc}/s) as well as late gadolinium enhancement (LGE) to predict functional improvement at follow-up (E_{cc}: area under the curve [AUC] 0.74, 95% confidence interval [CI]: 0.64 to 0.83; E_{cc}/s: AUC: 0.82, 95% CI: 0.72 to 0.89; LGE >75%: AUC: 0.85, 95% CI: 0.77 to 0.92). In a comparison of receiver operating characteristics curves, LGE was significantly different than E_{cc} but not E_{cc}/s ($p = 0.32$ vs. $p < 0.05$, respectively).

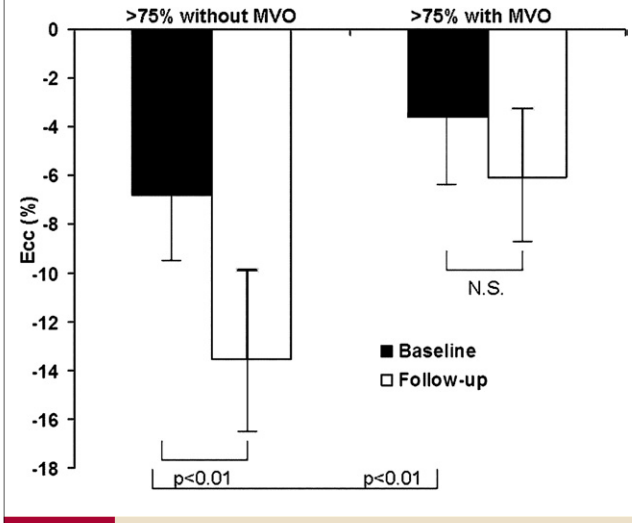

Figure 3 Influence of MVO on E_{cc}

Comparison of peak systolic strain values of LGE segments with and without signs of MVO. E_{cc} was even more impaired in segments with MVO compared with segments without MVO ($p < 0.01$). Segments with MVO showed no significant increase at follow-up, whereas segments without MVO improved ($p = 0.2$ and $p < 0.01$, respectively). MVO = microvascular obstruction; other abbreviations as in Figure 2.

Reproducibility. A total of 180 segments were evaluated for interobserver variability of E_{cc} and E_{cc}/s determined by SENC. The interobserver variability for both E_{cc} and E_{cc}/s was excellent (ICC for E_{cc} 0.91, ICC for E_{cc}/s 0.89).

Discussion

To our knowledge, this is the first study evaluating the value of systolic and diastolic deformation indexes assessed by SENC to predict persistent severe dysfunction at follow-up in patients after AMI. The findings of this study demonstrate that: 1) regional diastolic function provides similar accuracy for prediction of severe dysfunction at follow-up compared with LGE and is superior to regional systolic function; and 2) in segments with MVO, E_{cc} and E_{cc}/s showed even more functional compromise compared with transmural infarcted segments without MVO with no functional improvement at follow-up.

Prediction of persistent severe dysfunction. Identification of viable and nonviable segments in patients after AMI has important therapeutic and prognostic implications. Therefore, intensive work has been put into the development of noninvasive imaging methods to identify and quantify myocardial viability. Recently LGE has been proven to be the gold standard for assessment of viability (4,18). The predictive power of LGE in our study was similar to previous reports (6,18,19). Ichikawa et al. (18), for example, reported an AUC of 0.84 for LGE >75% comparable to our results (AUC: 0.85). Gerber et al. (3) reported slightly lower AUCs in the investigation of the accuracy of LGE in predicting improvement of regional myocardial function in patients after AMI.

In this study, we demonstrated that regional diastolic function, but not regional systolic function, assessed by SENC, is comparable to that assessed by LGE for prediction of functional recovery in patients after AMI. Recently gadolinium-induced nephrotic systemic fibrosis has limited

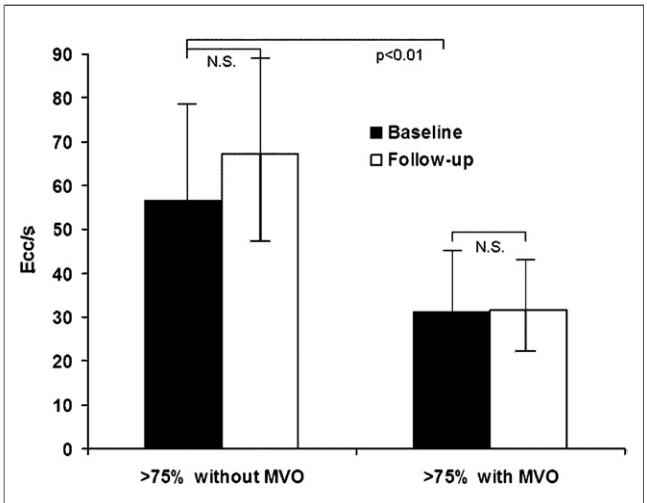

Figure 4 Influence of MVO on E_{cc}/s

Comparison of early diastolic strain rate values of LGE segments with and without signs of MVO. E_{cc}/s was significantly more impaired in segments with MVO compared with segments without MVO ($p < 0.01$), both showing no improvement at follow-up ($p = 0.99$ and $p = 0.6$). Abbreviations as in Figures 2 and 3.

the application of contrast agents in patients with renal insufficiency. Low-dose dobutamine stress cine MR imaging has been proven to be an alternative to LGE for prediction of functional recovery after AMI (19). However, the application of dobutamine directly after AMI can bear the risk of arrhythmias. Strain-encoded imaging is still a research tool; however, once this technique is implemented in the software of the scanner, the strain values could be provided online. This holds the advantage of saving scan time with no need for contrast agents. Therefore, it may be an alternative to LGE in the future for unstable patients after AMI, for which short scan times are desirable, or patients with renal insufficiency with contraindication to contrast agents.

The predictive value of regional diastolic function has been demonstrated before in echocardiographic animal studies. Park et al. (9) investigated 16 dogs after occlusion of the left anterior descending coronary artery or circumflex coronary artery and measured diastolic strain rate by Doppler echocardiography to predict functional improvement and found that diastolic strain rate was closely related to interstitial fibrosis and may be a promising novel index of myocardial viability, which is in line with our data. The close relationship between changes in strain rate and myocardial fibrosis has been also demonstrated before in patients with nonischemic fibrosis (20). Interestingly, in our study, systolic function showed more improvement than diastolic function at follow-up. Azevedo et al. (8), investigating regional systolic and diastolic function after AMI in dogs, also observed persistent regional diastolic impairment despite recovery of systolic function; however, there were no long-term follow-up data. A recent echocardiographic strain study demonstrated an increase in accuracy to identify reversible myocardial dysfunction by integration of myocardial deformation imaging and LGE in patients with chronic MI (21). We also found that in patients directly after AMI, a combination of LGE and E_{cc}/s achieved slightly better results but not significantly different than those produced by LGE or E_{cc}/s alone.

Influence of presence of MVO. Several studies have shown that MVO is associated with adverse cardiac remodeling and poor outcome and prognosis (22–24). The data derived from the present study demonstrate that segments with MVO demonstrate more impaired regional systolic and diastolic function compared with transmural infarcted segments without MVO, which may indicate more myocardial damage. Moreover, segments with MVO failed to show improvement of systolic and diastolic function at follow-up, which is in line with other studies.

Gerber et al. (3) investigated the value of early hypoenhancement on prediction of systolic functional recovery using MR tagging. They found a high positive predictive value and a high specificity in forecasting persistent dysfunction for segments with early hypoenhancement, which is at odds with our data. Azevedo et al. (8), investigating regional systolic and diastolic function in segments with MVO, found these segments also to display further compromise of systolic and diastolic regional function in an animal model than hyperenhanced segments. One explanation for this is that previous experimental and animal studies demonstrated that hypoenhanced myocardium within hyperenhanced myocardium represents necrotic tissue with microvascular damage and obstruction and therefore is more damaged than hyperenhanced myocardium without hypoenhancement.

SENC imaging for deformation imaging. Magnetic resonance tagging is the state of the art technique in MRI to assess myocardial function (25). However, MR tagging has some limitations such as diastolic fading of tags and suboptimal spatial and temporal resolution.

Recently other functional MR techniques, such as displacement encoding with stimulated echoes, phase-sensitive cardiac tagging, as well as SENC, have been introduced to overcome the limitations of tagging (11,12,26–28). In this study, we assessed regional systolic and diastolic function using SENC. Several studies have shown that SENC closely correlates to MR tagging and is able to assess strain and strain rate in healthy volunteers as well as in acutely and chronic infarcted patients (10,13,29,30). Compared with MR tagging, SENC is less affected by diastolic fading because RF pulses with ramped flip angles are applied to compensate for tag fading caused by longitudinal relaxation to maintain constant myocardial signal intensity throughout the cardiac cycle within acceptable breath-hold times (12). Therefore SENC provides improved interpretation of diastolic function.

Study limitations. First, we only included a small number of patients. Second, measured strain values were not exactly zero, not even in segments with MVO. This phenomenon may be explained by measurement of artifacts related to tethering from adjacent segments or noise artifacts. Third, the left ventricle on long-axis planes was divided into 12 segments for data analysis. It may appear that abnormal systolic and diastolic function near the apex or base are underestimated in some cases.

Conclusions

SENC allows characterization of myocardial tissue and assessment of myocardial viability in patients after AMI. Regional diastolic function analysis after AMI provides similar accuracy for prediction of persistent severe myocardial dysfunction at follow-up compared with LGE and is more precise than regional systolic function analysis. Therefore, regional diastolic function may serve as a new parameter for assessment of viability in patients after AMI.

Reprint requests and correspondence: Dr. Mirja Neizel, Department of Cardiology, Pulmology and Angiology, University Hospital Düsseldorf, Moorenstrasse 5, 40225 Düsseldorf, Germany. E-mail: mirja.neizel@med.uni-duesseldorf.de.

JACC Vol. 56, No. 13, 2010
September 21, 2010:1056–62

REFERENCES

1. Sanz G, Castaner A, Betriu A, et al. Determinants of prognosis in survivors of myocardial infarction: a prospective clinical angiographic study. N Engl J Med 1982;306:1065–70.
2. Meluzin J, Cerny J, Frelich M, et al. Prognostic value of the amount of dysfunctional but viable myocardium in revascularized patients with coronary artery disease and left ventricular dysfunction. Investigators of this Multicenter Study. J Am Coll Cardiol 1998;32:912–20.
3. Gerber BL, Garot J, Bluemke DA, Wu KC, Lima JA. Accuracy of contrast-enhanced magnetic resonance imaging in predicting improvement of regional myocardial function in patients after acute myocardial infarction. Circulation 2002;106:1083–9.
4. Kim RJ, Wu E, Rafael A, et al. The use of contrast-enhanced magnetic resonance imaging to identify reversible myocardial dysfunction. N Engl J Med 2000;343:1445–53.
5. Kramer CM, Rogers WJ Jr., Mankad S, Theobald TM, Pakstis DL, Hu YL. Contractile reserve and contrast uptake pattern by magnetic resonance imaging and functional recovery after reperfused myocardial infarction. J Am Coll Cardiol 2000;36:1835–40.
6. Choi KM, Kim RJ, Gubernikoff G, Vargas JD, Parker M, Judd RM. Transmural extent of acute myocardial infarction predicts long-term improvement in contractile function. Circulation 2001;104:1101–7.
7. Rogers WJ Jr, Kramer CM, Geskin G, et al. Early contrast-enhanced MRI predicts late functional recovery after reperfused myocardial infarction. Circulation 1999;99:744–50.
8. Azevedo CF, Amado LC, Kraitchman DL, et al. Persistent diastolic dysfunction despite complete systolic functional recovery after reperfused acute myocardial infarction demonstrated by tagged magnetic resonance imaging. Eur Heart J 2004;25:1419–27.
9. Park TH, Nagueh SF, Khoury DS, et al. Impact of myocardial structure and function postinfarction on diastolic strain measurements: implications for assessment of myocardial viability. Am J Physiol Heart Circ Physiol 2006;290:H724–31.
10. Korosoglou G, Youssef AA, Bilchick KC, et al. Real-time fast strain-encoded magnetic resonance imaging to evaluate regional myocardial function at 3.0 Tesla: comparison to conventional tagging. J Magn Reson Imaging 2008;27:1012–8.
11. Osman NF, Sampath S, Atalar E, Prince JL. Imaging longitudinal cardiac strain on short-axis images using strain-encoded MRI. Magn Reson Med 2001;46:324–34.
12. Pan L, Stuber M, Kraitchman DL, Fritzges DL, Gilson WD, Osman NF. Real-time imaging of regional myocardial function using fast-SENC. Magn Reson Med 2006;55:386–95.
13. Neizel M, Lossnitzer D, Korosoglou G, et al. Strain-encoded (SENC) magnetic resonance imaging to evaluate regional heterogeneity of myocardial strain in healthy volunteers: comparison with conventional tagging. J Magn Reson Imaging 2009;29:99–105.
14. Dewey M, Laule M, Taupitz M, Kaufels N, Hamm B, Kivelitz D. Myocardial viability: assessment with three-dimensional MR imaging in pigs and patients. Radiology 2006;239:703–9.
15. Peukert D, Laule M, Taupitz M, Kaufels N, Hamm B, Dewey M. 3D and 2D delayed-enhancement magnetic resonance imaging for detection of myocardial infarction: preclinical and clinical results. Acad Radiol 2007;14:788–94.
16. Edvardsen T, Rosen BD, Pan L, et al. Regional diastolic dysfunction in individuals with left ventricular hypertrophy measured by tagged magnetic resonance imaging—the Multi-Ethnic Study of Atherosclerosis (MESA). Am Heart J 2006;151:109–14.
17. Ennis DB, Epstein FH, Kellman P, Fananapazir L, McVeigh ER, Arai AE. Assessment of regional systolic and diastolic dysfunction in familial hypertrophic cardiomyopathy using MR tagging. Magn Reson Med 2003;50:638–42.
18. Ichikawa Y, Sakuma H, Suzawa N, et al. Late gadolinium-enhanced magnetic resonance imaging in acute and chronic myocardial infarction. Improved prediction of regional myocardial contraction in the chronic state by measuring thickness of nonenhanced myocardium. J Am Coll Cardiol 2005;45:901–9.
19. Motoyasu M, Sakuma H, Ichikawa Y, et al. Prediction of regional functional recovery after acute myocardial infarction with low dose dobutamine stress cine MR imaging and contrast enhanced MR imaging. J Cardiovasc Magn Reson 2003;5:563–74.
20. Weidemann F, Niemann M, Herrmann S, et al. A new echocardiographic approach for the detection of non-ischaemic fibrosis in hypertrophic myocardium. Eur Heart J 2007;28:3020–6.
21. Hoffmann R, Stempel K, Kuhl H, et al. Integrated analysis of cardiac tissue structure and function for improved identification of reversible myocardial dysfunction. Coron Artery Dis 2009;20:21–6.
22. Hombach V, Grebe O, Merkle N, et al. Sequelae of acute myocardial infarction regarding cardiac structure and function and their prognostic significance as assessed by magnetic resonance imaging. Eur Heart J 2005;26:549–57.
23. Wu KC, Zerhouni EA, Judd RM, et al. Prognostic significance of microvascular obstruction by magnetic resonance imaging in patients with acute myocardial infarction. Circulation 1998;97:765–72.
24. Baks T, van Geuns RJ, Biagini E, et al. Effects of primary angioplasty for acute myocardial infarction on early and late infarct size and left ventricular wall characteristics. J Am Coll Cardiol 2006;47:40–4.
25. Zerhouni EA, Parish DM, Rogers WJ, Yang A, Shapiro EP. Human heart: tagging with MR imaging—a method for noninvasive assessment of myocardial motion. Radiology 1988;169:59–63.
26. Aletras AH, Ingkanisorn WP, Mancini C, Arai AE. DENSE with SENSE. J Magn Reson 2005;176:99–106.
27. Aletras AH, Tilak GS, Natanzon A, et al. Retrospective determination of the area at risk for reperfused acute myocardial infarction with T2-weighted cardiac magnetic resonance imaging: histopathological and displacement encoding with stimulated echoes (DENSE) functional validations. Circulation 2006;113:1865–70.
28. Derbyshire JA, Sampath S, McVeigh ER. Phase-sensitive cardiac tagging—REALTAG. Magn Reson Med 2007;58:206–10.
29. Garot J, Lima JA, Gerber BL, et al. Spatially resolved imaging of myocardial function with strain-encoded MR: comparison with delayed contrast-enhanced MR imaging after myocardial infarction. Radiology 2004;233:596–602.
30. Neizel M, Lossnitzer D, Korosoglou G, et al. Strain-encoded MRI for evaluation of left ventricular function and transmurality in acute myocardial infarction. Circ Cardiovasc Imaging 2009;2:116–22.

Key Words: myocardial dysfunction ■ myocardial infarction ■ SENC.